

- [3] Y. K. Wang, K. C. Fan, and J. T. Horng, "Genetic-based search for error-correcting graph isomorphism," *IEEE Trans. Syst., Man, Cybern. B*, vol. 27, pp. 588–597, Aug. 1997.
- [4] A. D. J. Cross, R. C. Wilson, and E. R. Hancock, "Inexact graph matching using genetic search," *Pattern Recognit.*, vol. 30, no. 6, pp. 953–970, 1997.
- [5] M. Singh, A. Chatterjee, and S. Chaudhury, "Matching structural shape descriptions using genetic algorithms," *Pattern Recognit.*, vol. 30, no. 9, pp. 1451–1462, 1997.
- [6] P. N. Suganthan, E. K. Teoh, and D. P. Mital, "Pattern recognition by homomorphic graph matching using Hopfield neural networks," *Image Vis. Comput.*, vol. 13, no. 1, pp. 45–61, 1995.
- [7] W. H. Tsai and K. S. Fu, "Error-correcting isomorphisms of attributed relational graphs for pattern analysis," *IEEE Trans. Syst., Man, Cybern.*, vol. SMC-9, pp. 757–768, 1979.
- [8] W. E. L. Grimson, "On the recognition of curved objects," *IEEE Trans. Pattern Anal. Machine Intell.*, vol. 11, no. 6, pp. 632–643, 1989.
- [9] N. Ayache and O. D. Faugeras, "HYPER: A new approach for the recognition and positioning of two-dimensional objects," *IEEE Trans. Pattern Anal. Machine Intell.*, vol. PAMI-8, no. 1, pp. 44–54, 1986.
- [10] O. D. Faugeras and M. Berthod, "Improving consistency and resolving ambiguity in relaxation labeling," *IEEE Trans. Pattern Anal. Machine Intell.*, vol. PAMI-3, no. 4, pp. 412–424, 1981.
- [11] S. Gold and A. Rangarajan, "A graduated assignment algorithm for graph matching," *IEEE Trans. Pattern Anal. Machine Intell.*, vol. 18, pp. 309–319, Apr. 1996.
- [12] C. Peterson and B. Soderberg, "A new method for mapping optimization problems onto neural networks," *Int. J. Neural Syst.*, vol. 1, no. 1, pp. 3–22, 1989.
- [13] P. N. Suganthan, E. K. Teoh, and D. P. Mital, "Pattern recognition by graph matching using the Potts MFT neural networks," *Pattern Recognit.*, vol. 28, no. 7, pp. 997–1009, 1995.
- [14] J. J. Hopfield and D. W. Tank, "Neural computation of decisions in optimization problems," *Biol. Cybern.*, vol. 52, pp. 141–152, 1985.
- [15] S. Kirkpatrick, C. D. Gellat, and M. P. Vecchi, "Optimization by simulated annealing," *Science*, vol. 220, pp. 671–680, 1983.
- [16] R. Myers and E. R. Hancock, "Least commitment graph matching with genetic algorithms," *Pattern Recognit.*, vol. 34, pp. 375–394, 2001.
- [17] D. E. Goldberg, *Genetic Algorithms in Search, Optimization, and Machine Learning*. Reading, MA: Addison-Wesley, 1989.
- [18] J. Holland, *Adaptation in Natural and Artificial Systems*. Ann Arbor, MI: Univ. of Michigan Press, 1975.
- [19] P. N. Suganthan, E. K. Teoh, and D. P. Mital, "Optimal mapping of graph homomorphism onto self organizing Hopfield network," *Image Vis. Comput.*, vol. 15, pp. 679–694, 1997.
- [20] G. Stockman, "Object recognition and localization via clustering," in *CVGIP, Graph. Models Image Process.*, vol. 40, 1987, pp. 361–387.
- [21] N. Ansari and E. F. Delp, "On detecting dominant points," *Pattern Recognit.*, vol. 24, no. 5, pp. 441–451, 1991.

## Perceptually Stable Regions for Arbitrary Polygons

Jairo Rocha

**Abstract**—Zou and Yan [10] have recently developed a skeletonization algorithm of digital shapes based on a regularity/singularity analysis; they use the polygon whose vertices are the boundary pixels of the image to compute a constrained Delaunay triangulation (CDT) in order to find local symmetries and stable regions. Their method has produced good results but it is slow since its complexity depends on the number of contour pixels. This paper presents an extension of their technique to handle arbitrary polygons, not only polygons of short edges. Consequently, not only can we achieve results as good as theirs for digital images, but we can also compute skeletons of polygons of any number of edges. Since we can handle polygonal approximations of figures, the skeletons are more resilient to noise and faster to process.

**Index Terms**—Polygon skeleton, polygon Voronoi diagram, regular/singular region, stable region.

### I. INTRODUCTION

Decomposition into regular and singular regions and its application to skeletonization has been an important subject of research since the seminal papers [6], [8] of about ten years ago. We present in this paper the first method for regular/singular decomposition that works on any kind of polygon. Zou and Yan's method [10], that hereafter will be called ZYM, works only when the polygon nodes are very near each other so that they never have to be split to analyze the local symmetries. Rocha and Bernardino's method [7] works only when the edges are long so that a parallelism criterion can be robustly applied to characterize regular from singular regions. There are no other algorithms in the literature for polygon analysis that are rotationally invariant, that use no external parameters and that avoid protrusions in the skeleton. Our method gives as skeleton for a perfect rectangle only one axis, the longest one, in contrast with most methods, such as [4], which also give four short axes, one for each corner. Other methods that give only a line as the skeleton of a rectangle, e.g., [1], are pixel-based.

Our method can be understood as a modification of the medial axis (calculated by the Voronoi diagram) of the polygon using the *perceptually stable* regions used by ZYM. However, since the proposed method works on any kind of polygons, the computational cost can be reduced since it depends on the number of edges in the polygon contour. This number is a small number compared to the number of pixels, on which ZYM depends.

### II. BASIC DEFINITIONS OF VORONOI DIAGRAMS OF POLYGONS

Let us assume that we have a polygon possibly with polygonal holes. The polygon is defined by several sequences of oriented segments. In each sequence, called contour, two segments that follow each other are adjacent, and the first segment is adjacent to the last one. Also, the polygon interior is assumed to be on the left side of the segments. The Voronoi diagram of an arbitrary polygon has been studied by a number of people and can be computed in  $O(n \log n)$  time, where  $n$  is the number of polygon segments [2]. By their own definitions, it is also true

Manuscript received February 20, 2002. This work was performed as part of the Project CICYT DPI2002-2311-C03-02. This paper was recommended by Associate Editor X. Jiang.

J. Rocha is with the Department of Mathematics and Computer Science, University of the Balearic Islands, Palma de Mallorca, E07071 Spain (e-mail: jairo@uib.es).

Digital Object Identifier 10.1109/TSMCB.2003.808189

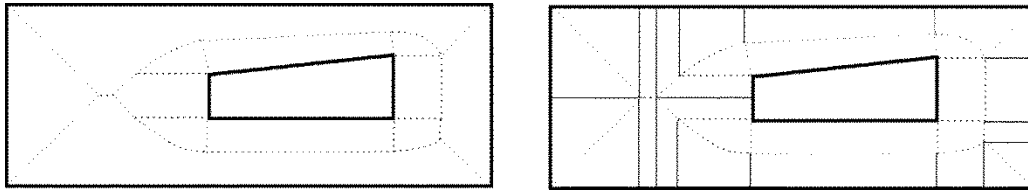


Fig. 1. Voronoi edges of a polygon (left). Projections of Voronoi points over their segments creating subsegments used for defining neighbor segments (right).

that the Voronoi edges for a polygon contain its *medial axis transform* (MAT), e.g., its skeleton in the most traditional sense of this term.

We will briefly recall some notation of Voronoi diagrams for line segments [3]. As usual, the polygon is assumed to be composed of open segments and vertex points, which are the elements of the polygon. Also, a polygon divides the plane into inside and outside points. If  $e$  is an element, the Voronoi region  $V(e)$  is the locus of inside points closest to element  $e$  than to any other element (inside points whose distance to a segment  $e$  is the same as its distance to one of the vertices of  $e$  are considered closer to the vertex). The boundary edges of a Voronoi region are called *Voronoi edges*. The vertices of the region are called *Voronoi points* (points adjacent to more than two regions). The Voronoi edges shared by the Voronoi regions of two polygon segments are portions of a bisectrix of the lines that contain the segments, while the Voronoi edges shared by a vertex and a segment are portions of a parabola. The Voronoi edges shared by two vertices are also straight lines.

A Voronoi region of a segment  $s$  has as boundary  $s$  itself and some Voronoi edges. The following observation is simple but very useful.

*Remark 1:* Let  $s$  and  $V(s)$  be a segment and its Voronoi region. Let  $P$  be a point on the boundary of  $V(s)$ . The line segment from  $P$  to  $s$  that is orthogonal to  $s$  is contained in  $V(s)$  or it is part of a Voronoi edge between  $V(s)$  and the Voronoi region of a vertex of  $s$ .

*Proof:* Consider the circle  $C$  centered in  $P$  and with a radius equal to the distance from  $P$  to  $s$ .

If  $C$  passes through one of the vertices,  $Q$ , of  $s$ , then all points in the segment  $PQ$  are also at equal distance to  $Q$  and  $s$ , so they are in the Voronoi edge between  $V(s)$  and  $V(Q)$ .

If  $C$  is tangent to  $s$ , let  $Q$  be the tangent point. If any point of the segment  $PQ$  is outside  $V(s)$  then there exists a point  $R$  in  $PQ$  that is in a Voronoi edge of  $V(s)$ ; consider a circle  $C'$  centered in  $R$  and tangent to  $s$ ;  $C'$  is also tangent at the point  $Q$ , and  $C'$  is completely contained in the circle  $C$ . Therefore, it is impossible that  $C'$  touches another polygon element. This contradiction implies that  $R$  cannot exist. •

Consider a point  $P$  on a Voronoi edge between two Voronoi regions associated to two segments. On each Voronoi region, consider the orthogonal projection of  $P$  on each segment; when we sweep the complete Voronoi edge by moving  $P$ , the orthogonal projections sweep the segments and define two subsegments, one on each segment, that are associated through the Voronoi edge.

Motivated by the previous statement, for each segment  $s$ , take the orthogonal projection over  $s$  of the Voronoi points adjacent to  $V(s)$ . In the rest of the paper, we will use the term polygon segments for the subsegments in which the original segments are divided according to the Voronoi diagram. Furthermore, we will work only with the new Voronoi diagram, associated with the new segments, which has some additional edges that divide old Voronoi regions into new ones. As we will see below, segments are naturally partitioned into subsegments according to their closest neighbor segments. For an example, see Fig. 1.

Given a segment  $s$ , let us consider  $V(s)$ . According to Remark 1, the orthogonal projection of a Voronoi point adjacent to  $V(s)$  over  $s$  is on the interior of  $s$  or is one of the vertices of  $s$ . However, it cannot be on the interior because polygon segments have already been divided according to these projections. Thus, Voronoi edges are projected on polygon vertices. As a result, the boundary of  $V(s)$  is made up of  $s$

itself, two Voronoi rectilinear edges orthogonal to  $s$  that lie over the vertices of  $s$ , and a Voronoi edge  $e_s$  that joins these two edges; one of the two orthogonal edges can be reduced to a point. In short,  $V(s)$  is bounded by maximum four, and minimum three edges. We have proved the following observation.

*Remark 2:* Given a segment  $s$ ,  $V(s)$  is bounded by  $e_s$  and maximum two rectilinear Voronoi edges orthogonal to  $s$ .

Given  $s$ ,  $e_s$  is shared with another Voronoi region. If this region is associated to a segment  $s'$ , then  $e_{s'} = e_s$  and it is a rectilinear edge. Given the distance constrains,  $V(s')$  is symmetrical to  $V(s)$  with respect to  $e_s$  and thus  $s$  and  $s'$  have the same length.

Given  $s$ , if the other Voronoi region is associated to a vertex  $v$ , then  $e_s$  is a parabolic edge, and  $v$  is unique because there is only one parabola that has  $s$  as directrix and that be adjacent to the Voronoi edges of  $V(s)$ .

*Definition 1: Neighbor Segments:* Two open polygon segments  $s_1$  and  $s_2$  are *neighbors* if  $e_{s_1} = e_{s_2}$ . In other words, their Voronoi regions share the Voronoi edge that is the bisectrix of the two segments.

If two segments are neighbors, we say that one is a neighbor of another and that they are neighbor segments. When two segments are neighbors, there is an interior circle that is tangent to both segments and that does not contain any point of other polygon elements. Notice also that each Voronoi edge has two and only two polygon elements associated to it.

Although in this paper we do not use the concept of *MAT skeleton* of a polygon, we recall that all Voronoi edges that are not adjacent to a concave polygon vertex (or a vertex with a straight angle) are part of the MAT skeleton.

### III. ORIGINAL POLYGON PARTITION

As we said before, a Voronoi edge can be a portion of bisectrix between polygon segments, a portion of a parabola between a polygon segment and a vertex, or a portion of a bisectrix between two polygon vertices. Thus, each Voronoi edge has two polygon elements associated to it as shown in Fig. 2.

For each pair of polygon elements associated to a Voronoi edge, we add the following interior segments: if the elements are two polygon segments  $AB$  and  $CD$  in the orientation given by the Voronoi edge, we add two new segments  $AC$  and  $BD$  (the segment  $AD$  is also added when we need to obtain a triangulation); if the elements are a vertex  $P$  and a polygon segment  $AB$ , we add the segments  $PA$  and  $PB$ ; and, finally, if the elements are the vertices  $P$  and  $Q$  we add the segment  $PQ$ .

The interior segments added do not intersect each other except in the boundaries because of two reasons: First, a polygon segment  $s$  shares the Voronoi edge  $e_s$  with only one polygon segment or vertex, and second, the vertex-vertex segments are added exactly in the same way as in the Delaunay triangulation, so the same basic Voronoi properties apply. Therefore, they form a partition of the polygon into triangles and trapezoids. Hereafter, we use the term *external edges* for the original polygon segments, and *internal edges* for the added segments (see Fig. 3 for an example) A partition element has one of the following

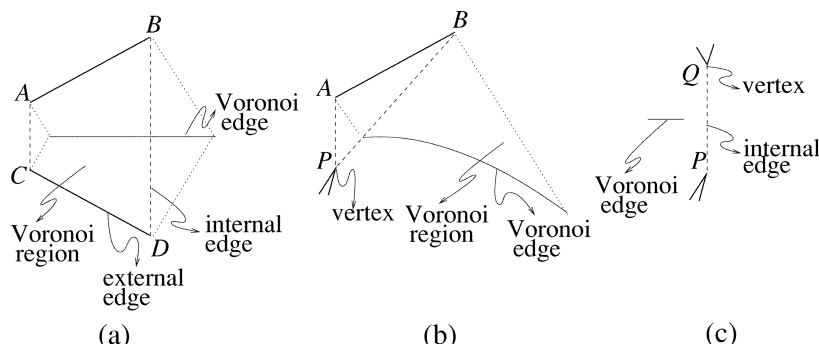


Fig. 2. Three situations for generating interior edges: (a) segment-segment; (b) segment-vertex; and (c) vertex-vertex.

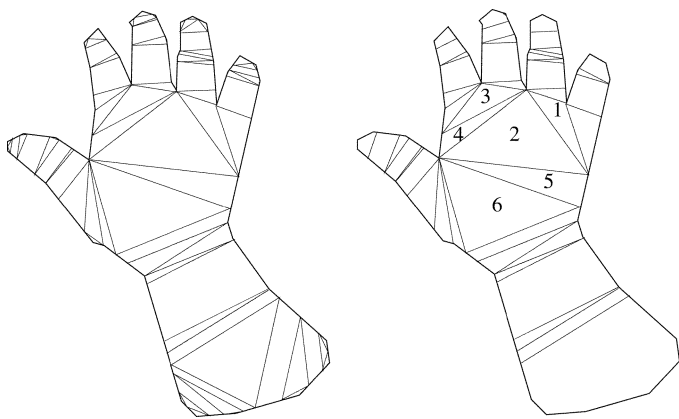


Fig. 3. Internal edges of a polygon (left). Stabilization of end regions (right).

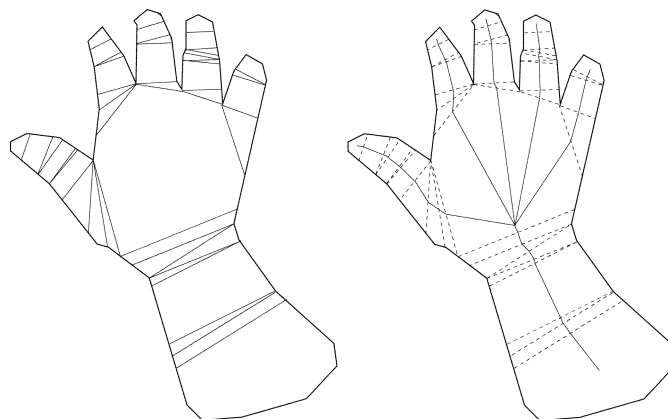


Fig. 4. Stabilization of intersection regions (left). Skeleton (right).

types: a *trapezoid* (generated by two neighbor segments and two internal edges), a *parabola triangle* (generated by an external edge and two internal edges from this to a polygon vertex), and a *totally internal triangle* (generated by three internal edges).

The partition is a triangulation if the trapezoids formed by neighbor segments are divided, as explained above. However, to obtain the final skeleton, regions will be merged so there is no need to begin with a triangulation.

#### IV. UNSTABLE REGIONS

A *region* is a connected set of triangles. As in ZYM, we classify the regions according to the type of edges that make up their boundary. An *isolated* region has no internal edges in its boundary; an *end* region has one internal edge; a *regular* region has two internal edges, and an *intersection* region has more than two internal edges. A *singular* region is either an end or an intersection region. The original regions defined above will be grouped to define the final regular and singular regions.

We now define when an end region and an intersection region are stable, modifying the criteria of ZYM to get very similar results at the highest resolution level.

An end region  $R$  has one adjacent region  $S$  that shares the internal edge  $e$  with  $R$ . Let  $w$  be the maximum length among the internal edges of  $S$ , if  $S$  is an intersection region. Otherwise,  $w$  is the length of  $e$ . The circle centered in the midpoint of  $e$  and whose diameter is  $\sqrt{2}w$  is called the *characteristic circle* of  $R$ .

**Definition 2:** An end region is *unstable* if no part of it lies outside its characteristic circle.

Zou and Yan [10] give a perceptual motivation of this definition: A stroke (ribbon) should have a length greater than its width; the shortest stroke is a square of side  $w$ , that can be enclosed in a circle of diameter  $\sqrt{2}w$ ; if a region  $R$  has an edge  $e$  as border with another region but it

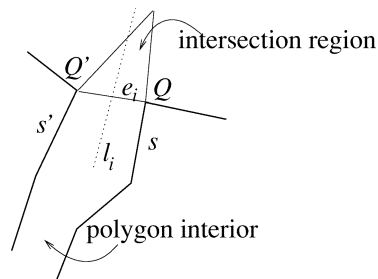


Fig. 5. Local orientation of a region adjacent to an intersection region.

can be enclosed in this small circle, then we can say that is shorter than the smallest possible stroke; thus, a stroke that is not at least half of it outside the adjacent region is considered a protrusion and not a stroke by itself. We just add that according to our experiments the definition allows to eliminate easily small branches, sometimes too many. However, we do not change it in order to be able to compare the results.

An intersection region has  $n$  interior edges  $e_1, \dots, e_n$ , and it is adjacent to  $n$  regions, which are not intersection regions; otherwise, adjacent intersection regions are merged.

The endings of an edge  $e_i = QQ'$  lie on the polygon contour (that leaves the polygon interior on its left); assume that  $QQ'$  leaves the intersection region on its right (see Fig. 5). Consider  $s$  the polygon segment adjacent to  $Q$  and before it in the contour order, and  $s'$  the polygon segment adjacent to  $Q'$  and after it; assume that the length of both  $s$  and  $s'$  is larger than half of the length of  $e_i$ ,  $d_i/2$ . The bisectrix  $l_i$  of these two segments is defined to be the local orientation of the region adjacent to  $e_i$ . If  $s$  (or  $s'$ ) is smaller than required, a point  $X$  on the contour located at a distance over the contour equal to  $d_i/2$  is found before (after)  $Q$  ( $Q'$ ) and the direction between  $Q(Q')$  and  $X$  is used to get the bisectrix  $l_i$ , instead of  $s(s')$ . The reason behind this required

distance is to avoid using segments that are too small to estimate the orientation of the entering stroke. The distance assumes, again, that a stroke should have a length greater than its width and that it is at least half of it outside of the intersection region.

We define the *characteristic skeleton point*  $P$  of the intersection region as the point interior to the polygon that makes the distance to all  $l_i, i = 1, \dots, n$  a minimum.

*Definition 3:* An intersection region is *unstable* if its characteristic skeleton point lies outside it.

Again, Zou and Yan give a perceptual motivation of the previous definition based on the natural orientation of crossing strokes of a line figure: If the “true” orientation of the strokes before entering an intersection is known, the “true” stroke intersection point is the intersection of the prolongation of the skeleton axes in their orientations; the “true” intersection region should be centered around this point. Therefore, the region in which the point closest to all lines lies is merged into the candidate intersection region.

Our definition differs from ZYM in two ways: First, they define  $w$ , for the characteristic circle, as the maximum length among the internal edges of the adjacent region  $S$ , for all kinds of regions; we do not use the maximum for regular regions because our regions are, in general, large, and the length of the furthest edge is not related to the context of region  $R$ . Second, ZYM does not define precisely the local orientation of a region (ribbon) adjacent to the intersection region: An average of the local contour orientation of the ribbon near the intersection region is used, but the number and position of pixels used for the average is not given. For these reasons, our solution may differ a bit in some figures. However, our main area of interest is at low resolutions, in which segments give a good orientation of the polygon contour, if the polygon approximation finds good corners and straight lines in the figure. Therefore, we prefer the simple and precise definition of local orientation given in the paragraph above.

An end region that is unstable is merged to a part of its adjacent region, as it is defined below. An intersection region that is unstable is merged to a part of the adjacent region that is the nearest to its characteristic skeleton point. This merging process is called *stabilization*. After an end region is merged, it is possible that the new region is not an end region. However, during the merging process end regions are processed prior to intersection regions.

ZYM always merges a region with a complete adjacent region; since the external edges of their regions are usually small, the area added to the region is also small; this is not the case with our regions so we add only part of the region, as described in the next paragraph.

When an end region  $R$  is merged with an adjacent region  $S$ , there are three cases for the region  $S$ , according to the type of the triangle  $T$  in  $S$  adjacent to  $R$ : if  $T$  is singular,  $S$  is merged completely to  $R$ . If the triangle  $T$  is regular, let  $e$  be the internal edge common to  $R$  and  $S$  (see Fig. 6). If  $T$  is part of a trapezoid, we find a new edge  $e'$  parallel to  $e$  with its extremes lying on the neighboring segments, as close as possible to  $e$  and that satisfies the following condition: the new region of  $R$  merged with the subregion between  $e$  and  $e'$  is stable. If  $e'$  does not exist, the trapezoid is completely merged to  $R$ . If the triangle  $T$  is a parabola triangle with external edge  $f$  and vertex  $V$ , we find a new segment  $e'$  from  $V$  to a point lying on  $f$  as close as possible to  $e$  and such that the new region of  $R$  merged to the subregion between  $e$  and  $e'$  be stable. If  $e'$  does not exist,  $T$  is completely merged to  $R$ .

For an intersection region  $R$ , if the characteristic skeleton point lies in a region  $S$  that is adjacent to  $R$ , part of  $S$  is added so it includes the characteristic point  $P$  as follows: If the region  $S$  is an end region, all  $S$  is merged to  $R$ . Otherwise, let  $e$  be the internal edge common to  $R$  and  $S$ , and  $T$  the triangle in  $S$  adjacent to  $R$ . If  $T$  is part of a trapezoid, we find a new segment  $e'$  parallel to  $e$ , whose extremes lie on the neighboring segments and that passes through the point  $P$ ; we

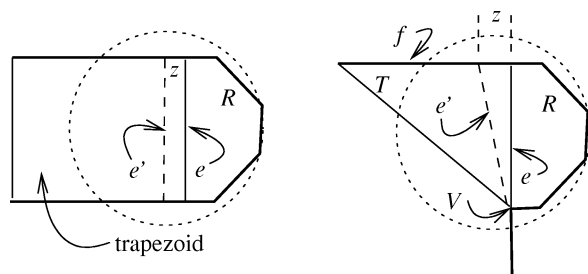


Fig. 6. Merging of an end region with a trapezoid, and with a parabola triangle.

merge the subregion between  $e$  and  $e'$  to  $R$ . If  $T$  is a parabola triangle, we find a segment  $e'$  from  $V$  to a point over the external edge of  $T$  that passes through  $P$ ; we merge the subregion between  $e$  and  $e'$  to  $R$ . In both cases, the characteristic point is moved to the center of the edge  $e'$ ; otherwise, when making the skeleton, the line between the center of  $e'$  and the characteristic point situated also over  $e'$  would cause a step line in the skeleton, as it does in ZYM.

If the characteristic point  $P$  of an intersection region  $R$  does not lie on a region adjacent to  $R$ , then the region  $S$  adjacent to  $R$ , that is on the shortest path from  $P$  to  $R$  within the polygon, is merged to  $R$ .

In the example shown in Figs. 3 and 4, first, the internal triangles 1 and 2 are merged; second, the characteristic point of triangle 3 is outside it, so it is merged to triangle 4, which is then merged to the region of triangle 2; the region of triangles 1, 2, 3, and 4 is not stable so it is merged to triangle 5, which is again merged to its adjacent internal triangle 6. The whole region is stable.

Now, some words are needed on how to calculate the subregions described in the previous paragraphs. The subregion to be merged to an intersection region are completely defined by its characteristic skeleton point position. On the other hand, for an end region, the subregion to be merged should be taken as small as possible, so that the new region is stable. Below we explain a simple optimization problem to find it.

Let  $T$  be the triangle adjacent to the end region  $R$ . If  $T$  is part of a trapezoid, the distance that should be a minimum is the distance  $z$  between the two parallel edges  $e$  and  $e'$ . The diameter and the center of the new characteristic circle can be expressed linearly in terms of  $z$ ; for each vertex of  $R$ , the constraint that it should be outside the circle is quadratic, so the whole problem is solved analyzing a quadratic polynomial in  $z$  for each vertex of  $R$ . If  $T$  is a parabola triangle, the distance that should be a minimum is the distance  $z$  between the vertex of  $e$  different from  $V$  and the point on  $f$  that defines the edge  $e'$ ; again, the diameter and the center of the new characteristic circle can be expressed linearly in terms of  $z$ , although the constants are more complex; again, the quadratic polynomial roots solve the problem.

Skeletons are found following the same ZYM's algorithm: the skeleton of a regular triangle or trapezoid is the straight line segment connecting the midpoints of the two internal edges of the region; if the regular region is neither a triangle nor a trapezoid, the skeleton is defined as if it were an intersection region; for intersection regions, the skeleton is a set of straight line segments connecting its characteristic skeleton point to the internal edge midpoints; the skeleton of an end region connects its centroid to the midpoint of its internal edge.

## V. RELATION TO CONSTRAINED DELAUNAY TRIANGULATION (CDT)

The *constrained Delaunay triangulation (CDT)* of a polygon is a triangulation where the circumcircle of each triangle does not contain in its interior any other vertex of the polygon which is visible from all the vertices of the triangle. CDTs are used in ZYM as a tool to approximate the medial axis. Skeletons found using CDT become exact when the contour segment lengths approach zero.

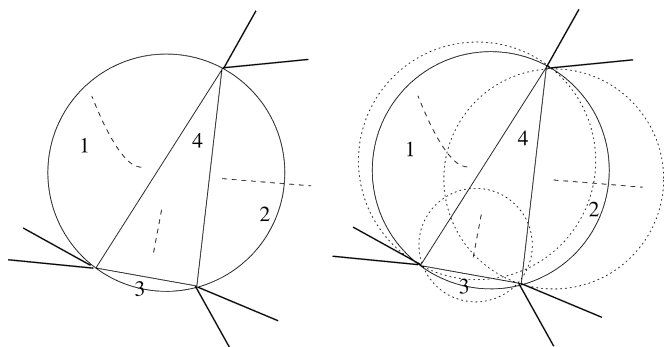


Fig. 7. Triangle made of internal edges. Circumcircle zones 1, 2, and 3 are covered by circles that are known to be vertex-free.

Therefore, they use the smallest possible segments: the straight lines connecting two contour pixels.

We propose to use a Voronoi diagram for segments to find the medial axis and, after some adjustments, perform their same analysis on singular regions. We want to show in this section that for a polygon with very small segments (i.e., at high resolution), the triangulation we find is very close to CDT. This result should be obvious considering what was said in the previous paragraph, but the explicit analysis helps clarify the relationship between the two methods.

Given a polygon, our method first splits the original polygon segments according to the Voronoi points (i.e., segments are split into neighbor segments); thus, the new polygon has new vertices. In the next step, it introduces internal edges that generate a partition of the polygon interior. We will show that the internal edges we add are exactly the same segments introduced by a CDT of the new polygon. Therefore, the regions that both algorithms work with are the same and the results would be the same.

However, their algorithm does not split the original segments. It relies on the fact that the segments are small so that a new vertex useful to find an exact axis should not be far away from an original vertex. On the other hand, new vertices sometimes coincide with the old ones even in our algorithm implementation according to the precision level used. In short, at a high resolution, it is true that the CDT is a tool to find skeletons very close to the exact ones. Our method works even if the segments are longer while their method breaks down.

For paper limitations, we will give just a sketch of the proof that our edges form a CDT of the new polygon.

*Remark 3:* A triangle made up of external and internal edges of a polygon with no other edges in its interior is part of the CDT of the polygon.

*Proof:* There are four basic cases: 1) if the triangle is totally internal; 2) if it is a parabola triangle; 3) if it is half of trapezoid; and 4) if it has more than one external edge.

*Case 1:* Consider a triangle with no edges in its interior and whose edges are made up of internal edges. There are different sub-cases according to how each internal edge was generated. An internal edge can be generated in one of three situations for its Voronoi edge: vertex-vertex, vertex-segment, or segment-segment situation.

The circumcircle of the triangle can be divided into four zones: three zones exterior to the triangle and adjacent to each interior edge, and the triangle itself. As suggested by Fig. 7, each exterior zone adjacent to an internal edge is covered by a circle centered on the corresponding Voronoi edge that passes through the internal edge vertices; this circle exists no matter what type of Voronoi edge is considered. Since this circle does not contain any other contour point of the polygon because of the basic properties of the Voronoi edges, then the zone does not contain any vertex either. By hypothesis, the triangle zone has no

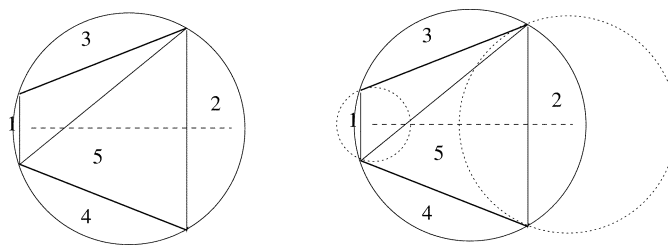


Fig. 8. Triangle that is part of a trapezoid made by two neighboring segments. The circumcircle contains all of the trapezoid and each zone is covered by a circle or it is not visible from all vertices.

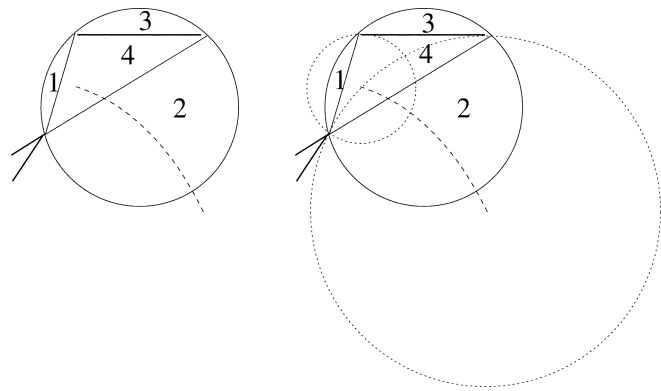


Fig. 9. Triangle that is generated in the parabolic Voronoi edge situation. Zones 1 and 2 are covered by circles that are vertex-free and zone 4 is not visible from all vertices.

other edges either, so the whole circumcircle does not contain any other vertex.

*Case 2:* If the triangle contains an exterior edge that is a neighbor segment, then the other two interior edges of the triangle are an edge and a diagonal of a trapezoid formed by the neighbor segments and the internal edges added, as shown in Fig. 8. The circumcircle can be divided into five zones. As suggested by this figure, zone 1 and zone 2 are covered by circles centered at the extreme of the Voronoi edge and tangents to the segments; hence, these two zones have no other vertices inside. Points inside zone 5 can be covered by maximal circles interior to the trapezoid and centered in the Voronoi edge. Finally, zone 3 and 4 are not visible from all the triangle vertices, so they do not matter.

*Case 3:* For the parabola triangle, its circumcircle can be divided into four zones. As suggested by Fig. 9, zone 1 and zone 2 are covered by circles centered at the extreme of the parabolic edge, tangents to the segment and that pass through the vertex, and therefore they do not contain any other polygon vertex. Zone 3 is the triangle interior which has no vertices, and zone 4 is not visible from all triangle vertices.

*Case 4:* If the triangle contains two external edges, then two of the edges are adjacent, and therefore, they are neighboring segments, so this is a degenerated situation of case 2 above, in which the trapezoid is reduced into a triangle that is an end region.

If the triangle has the three external edges, then it is a disconnected region and the circumcircle zone exterior to the triangle is not visible from all vertices. •

## VI. COMPARATIVE EXPERIMENTS

We test two conjectures. First, our results should be very similar to the ones yield by ZYM when the input polygon vertices consists of the image pixels. Second, when polygonal approximations are used, skeletons should change smoothly and the computational time should be reduced greatly.

TABLE I  
EXECUTION TIME FOR DIFFERENT NUMBER  
OF SEGMENTS IN THE POLYGON

Shape	approx.	segments	time
human	0	ZYM	12.50
	0	1232	132.50
	2	117	3.43
	4	46	1.05
hand	0	1056	97.51
	2	77	1.81
	4	43	0.94
cow	0	1950	383.40
	2	152	5.40
	4	83	2.06
spoon	0	789	68.90
	2	50	1.08
	4	18	0.49
sword	0	889	81.50
	2	72	1.49
	4	29	0.71
bottle	0	851	80.80
	2	48	1.04
	4	21	0.66

In our test we use a Pentium at 199 MHz. For simplicity, we use a slow but easy implementation of the Voronoi diagram calculation; for a new excellent implementation, the reader is referred to [2], which can handle thousands of segments per second with high precision with a comparable CPU. In the average, 86% of the time is consumed by our Voronoi diagram calculation. We extract the same unelongated images used by ZYM with a height of 500 pixels each. We use the polygonal approximation method described in [5] that requires an error parameter: the maximum distance in pixels from a contour pixel to the polygon edge that approximates it. We use the unelongated images because they are the most difficult ones: they have big singular regions.

The results are summarized in Table I (the second column is the parameter of the polygonal approximation; the third column is the number of segments in the polygonal approximation, except the first row which is for the ZYM data; the fourth column is the CPU time in seconds, ZYM uses a Pentium at 166 MHz), and the output is shown in Fig. 10.

There is no visible difference between the top row of Figs. 10 and 11 which has the original ZYM results and our results in the second row at our highest polygon resolution. As expected, CDTs allow us to calculate a very good approximation of the Voronoi diagram. Also, the variations in the criteria used to calculate stable regions do not affect the skeletons because both methods try to find the same type of regions. For the "human" image, the execution time of the proposed method is more than ten times greater than ZYM's for the highest resolution even though their images have a height of 1391 pixels (see the first two rows of Table I; the only ZYM's execution time available is for the "human"). This is due to the fact that Voronoi regions of segments are intrinsically more complex to find than CDTs and that we use a simple but inefficient implementation. Using better implementations (e.g., [2]), execution times could surely be reduced.

Nevertheless, the main point of the proposed method is that a large reduction is possible: for the second polygonal approximation level (a maximum distance of two pixels from a contour pixel to its corresponding segment) our method is almost four times faster than ZYM and, more importantly, 40 times faster than at the previous resolution; the differences in the skeleton are difficult to see. At the lowest approximation level, the proposed method is three times faster; at this level the skeleton segments are easier to see (see Figs. 12 and 13), so that the skeleton is not as smooth as the original one. The "cow" has lost a small branch near the ears because the

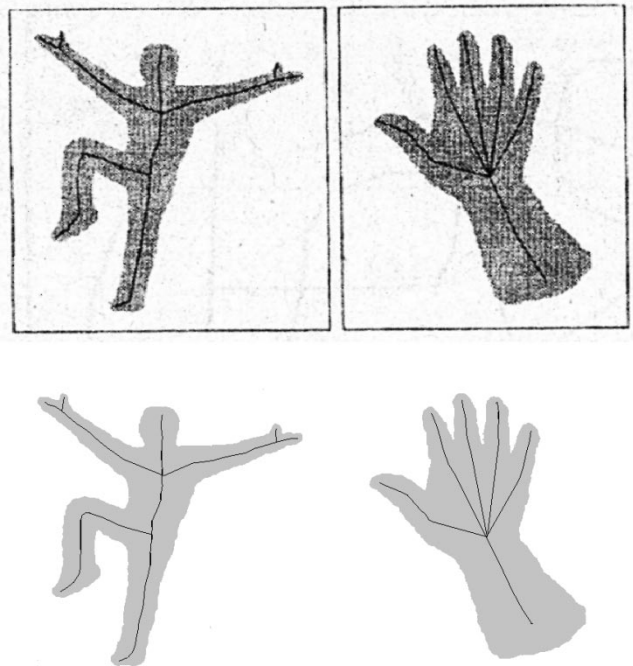


Fig. 10. ZYM results (top row). Proposed method results for the highest resolution level (bottom row).

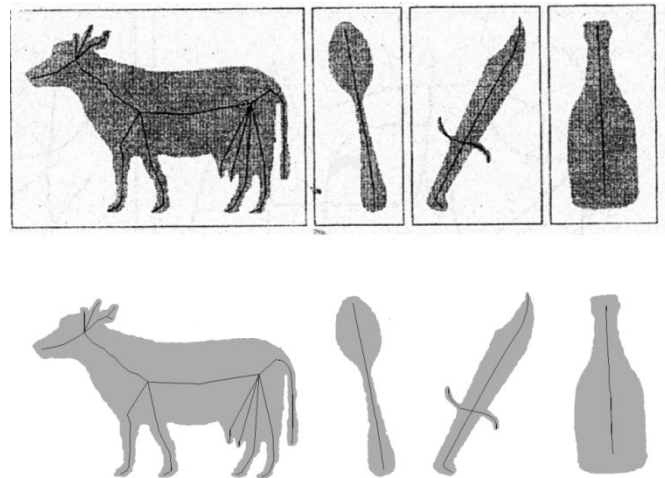


Fig. 11. ZYM results (top row). Proposed method results for the highest resolution level (bottom row).

polygonal approximation has smoothed the original protrusion; still, the proposed method is very useful for recognition applications.

We draw the reader's attention to the good skeleton degradation and the big improvement in computational time caused by the polygon size reduction.

Fig. 14 shows some results on elongated shapes in which a rough polygonal approximation is used. The final skeletons avoid most of spurious branches. Some of them remain like the one pointed by an arrow in the second character; "necks" can be eliminated by adding a rule suggested in [9]: It is possible to define the length of a sequence of adjacent regular regions as the length of its skeleton added to the distance to the characteristic skeleton points or centroids of adjacent singular regions; if the length of a sequence of regular regions is shorter than its average width, the sequence is merged into its adjacent singular regions. We have tried this rule and it works very well on a character data base. However, this rule would eliminate thick regions in human

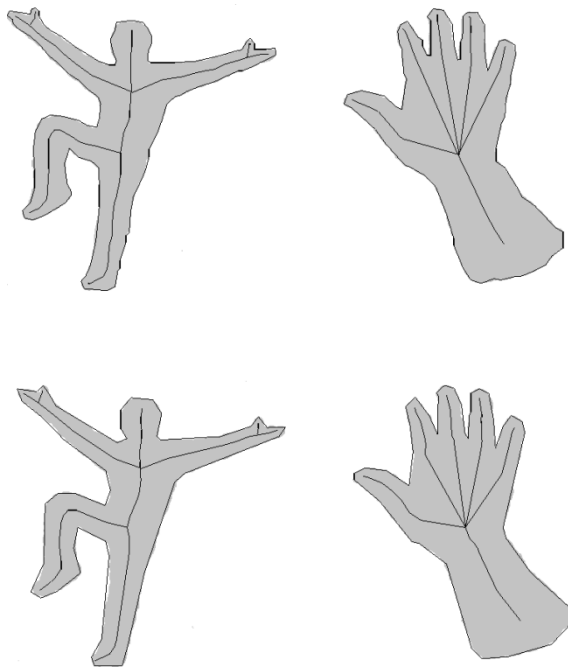


Fig. 12. Proposed method results for a medium resolution level (top row). Proposed method results for a low resolution level (bottom row).

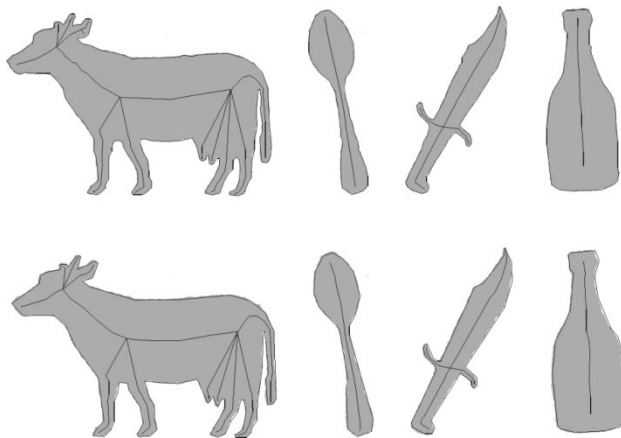


Fig. 13. Proposed method results for a medium resolution level (top row) and for a low resolution level (bottom row).

or animal like shapes. Therefore, the skeleton extraction is application dependent but the region partition is a good instrument to begin the skeleton analysis.

The same isolated regular triangle of the previous example shows another source of trouble: This triangle by itself is considered as a ribbon that enters into an intersection region; the local orientation of this ribbon cannot be estimated reliably because the segments that are used to calculate the orientation are out of the context of the triangle; the angle between these segments can be even greater than  $90^\circ$  so the bisectrix orientation between them is not robust. Fortunately, the troublesome case is identified by these two conditions: short isolated regular region and a large angle between the segments used for finding its local orientation. In this case, the local orientation importance of the region should be smaller than the the corresponding importance of other regions entering an intersection.

The reader should notice that the partition and skeletons shown in this challenging figure are very useful for OCR analysis.

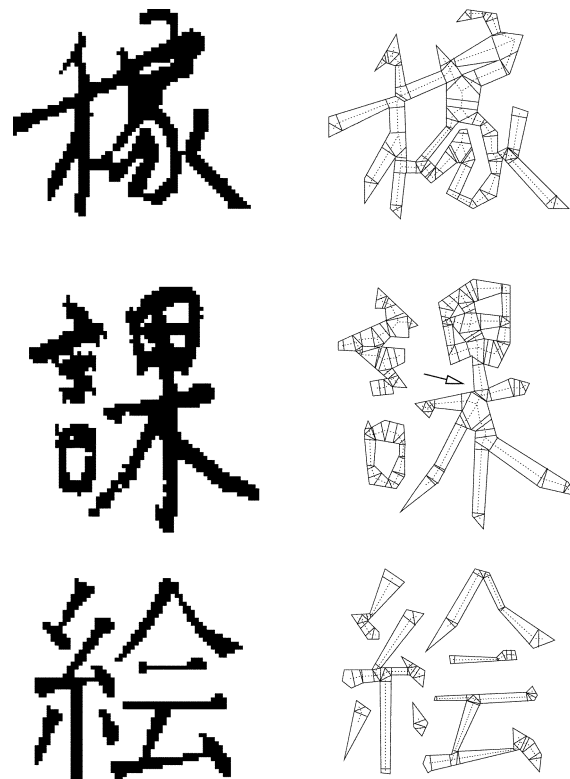


Fig. 14. Stable regions and skeletons for Kanji characters.

### VII. CONCLUSION

This paper extends the perceptual stability definitions of [10] to arbitrary polygons. The proposed method maintains the skeleton properties of its predecessor but it can be applied to arbitrary polygons.

Our tests show the possibility of greatly reducing the computational costs in recognition applications that do not require high resolution. More importantly, this paper shows a rotationally invariant, parameter free regular-singular analysis of arbitrary polygons, that inheres to the good results already proven by [10].

### REFERENCES

- [1] M. Frucci and A. Marcelli, "Line representation of elongated shapes," in *Computer Analysis of Images and Patterns*, V. Hlavac and R. Sara, Eds. Prague, Czechoslovakia, Sept. 1995, pp. 643–648. LNCS 970.
- [2] M. Held, "VRONI: An engineering approach to the reliable and efficient computation of Voronoi diagrams of points and line segments," *Comput. Geometry: Theory and Applicat.*, vol. 18, no. 2, pp. 95–123, 2001.
- [3] D. Lee and R. Drysdale, "Generalization of Voronoi diagrams in the plane," *SIAM J. Comput.*, vol. 10, pp. 73–87, Feb. 1981.
- [4] R. L. Ogniewicz and O. Kübler, "Hierarchic Voronoi skeletons," *Pattern Recognit.*, vol. 28, no. 3, pp. 343–359, 1995.
- [5] T. Pavlidis, *Algorithms for Graphics and Image Processing*. Rockville, MD: Computer Science, 1982.
- [6] T. Pavlidis and D. Lee, "Residual analysis for feature extraction," in *From Pixels to Features*, J. C. Simon, Ed. Amsterdam, The Netherlands: North-Holland, 1989, pp. 219–227.
- [7] J. Rocha and R. Bernardino, "Singularities and regularities via symmetrical trapezoids," *IEEE Trans. Pattern Anal. Machine Intell.*, vol. 20, pp. 391–395, Apr. 1998.
- [8] J. C. Simon, "A complementary approach to feature detection," in *From Pixels to Features*, J. C. Simon, Ed. Amsterdam, The Netherlands: North-Holland, 1989, pp. 229–236.
- [9] T. Suzuki and S. Mori, "Structural description of line images by the cross section sequence graph," *Int. J. PRAI*, vol. 7, no. 5, pp. 1055–1076, 1993.
- [10] J. Zou and H. Yan, "Skeletonization of ribbon-like shapes based on regularity and singularity analysis," *IEEE Trans. Syst., Man, Cybern. B*, vol. 31, pp. 401–407, June 2001.